We are IntechOpen, the world's leading publisher of Open Access books Built by scientists, for scientists

4,800
Open access books available

122,000
International authors and editors

135M
Downloads

Our authors are among the

154
Countries delivered to

TOP 1%
most cited scientists

12.2%
Contributors from top 500 universities

CLARIVATE ANALYTICS BOOK CITATION INDEX INDEXED

WEB OF SCIENCE™

Selection of our books indexed in the Book Citation Index in Web of Science™ Core Collection (BKCI)

Interested in publishing with us?
Contact book.department@intechopen.com

Numbers displayed above are based on latest data collected.
For more information visit www.intechopen.com

Chapter 5

Biaxial Tensile Strength Characterization of Textile Composite Materials

David Alejandro Arellano Escárpita, Diego Cárdenas, Hugo Elizalde, Ricardo Ramirez and Oliver Probst

Additional information is available at the end of the chapter

http://dx.doi.org/10.5772/48105

1. Introduction

Woven architecture confers textile composites (TC) multidirectional reinforcement while the undulating nature of fibres also provides a certain degree of out-of-plane reinforcement and good impact absorption; furthermore, fibre entanglement provides cohesion to the fabric and makes mould placement an easy task, which is advantageous for reducing production times [1]. These features make TC an attractive alternative for the manufacture of high-performance, lightweight structural components. Another interesting feature of TC is that they can be entangled on a variety of patterns, depending of the specific applications intended. Despite the wide interest of textile composites for industry and structural applications, most of the research efforts for strength characterization has focused on unidirectional composites (UDC), resulting in a large number of failure theories developed for UDC (around 20, as inferred from the conclusions of the World-Wide Failure Excercise (WWFE) [2]); some of the most popular failure models are used indistinctly for UDC and TC: most designers use Maximum Strain, Maximum Stress, Tsai-Hill and Tsai-Wu both for UDC or TC as stated in reference [3], despite the fact that none of the aforementioned failure criteria has been developed specifically for TC, which has led to use of high safety factors in critical structural applications to overcome associated uncertainties [4]. The most successful approaches to predict TC strength are based on phenomenological modeling of interactions between constituents at different scales (matrix-yarn-fiber), providing new insight into TC failure mechanisms. However, the implementation of phenomenological models as design tools is considerably more complex than that of traditional failure criteria, while still exhibiting significant deviation from the scarce experimental data [5] available. This scarcity of experimental data to validate or reject failure theories continues to be a major obstacle for improving TC models. Recent investigations reporting biaxial tensile strength tests in 2D-

triaxial TC employing tubular specimens suggested that the failure envelope predicted by the maximum strain criterion fits the experimental data in the tension-tension (T-T) quadrant [6] fairly well. Other tests performed on cruciform specimens indicated that the maximum stress criterion is more adequate [5]; however, the authors of ref. [5] expressed some concerns about the generality of the experimental methodology for the case of non quasi-isotropic lay-up configurations, such as the one studied in their work. In view of the lack of consensus for accurate TC strength prediction [7],[8], and as stated by researchers who participated in the World Wide Failure Exercises (WWFE) [2] more experimental data, better testing methods and properly designed specimens are needed to generate reliable biaxial strength models.

2. Biaxial testing review

Combined multi-axial strength characterization of composites is far from straightforward, as three basic elements are required: i) An apparatus capable of applying multi-axial loads, ii) a specimen capable of generating a homogeneous stress and strain field in a predefined gauge zone, producing failure inside this zone for correct strength characterization, and iii) a measurement system capable of acquiring the applied loads and resulting specimen strains. Although the general procedure is similar to that for uni-axial testing, significant complications arise due to the requirements outlined above; moreover, the required equipment is costly and available generally only at large specialized research centres. Regarding the specimens, the ability of generating a homogeneous multi-axial strain field inside a pre-specified gauge zone is not straightforward mainly due to geometric stress concentrations. Finally, the data acquisition system requires a free surface in order to perform direct measurements. In practice these factors limit the number of combined loads that can be applied to a single specimen to only two, although some researchers have proposed apparatuses designed to apply tri-axial loads, albeit at the expense of limiting the access for full field strain measurements. Efforts on multi-axial testing have been disperse and rather unsuccessful in defining adequate testing methodologies, as evidenced by the lack of standardization by international organisms which have otherwise generated well-known standards for uni-axial characterization of composites, such the ASTM D3039 (standard testing procedures for obtaining tensile properties of polymer matrix composites), British Standard: BS 2782: Part 3: Method 320A-F: Method for obtaining mechanical properties of plastics, BS EN ISO 527 Part 5: Plastics. Determination of tensile properties and test conditions for unidirectional fibre-reinforced plastic composites, CRAG (Composite Research Advisory Group) Test Methods for the Measurement of the Engineering Properties of Fibre Reinforced Plastics, Standard ASTM D6856: Testing procedures for textile composite materials, Japanese Industrial Standard JIS K7054: Tensile Test Method for Plastics Reinforced by Glass Fibre, Russian Standards GOST 25.601-80: Design Calculation and Strength Testing Methods of mechanical testing of polymeric composite materials. In brief, there exist at least seven standards for tensile uni-axial characterization, while none specific standard for bi-axial testing. This demonstrates the need for developing biaxial

testing methodologies. In this chapter a review is presented of the state of the art of multi-axial testing with emphasis on biaxial tensile specimens, testing machines and data measurement systems. The reasons for concentrating on biaxial loads are: i) The complexity of testing systems increases considerably with the the number of independent applied. ii) Most structural applications of composites uses thin skins, resulting in shell structures, in which the thickness of the laminates is significantly smaller than the other dimensions. One characteristic of shell structures is that buckling failure modes are the limiting factors in the case compressive loads [9]; consequently, the structural strength depends little on the materials strength and mostly on the geometry and stiffness. On the other hand, when tensile loads are applied to shell, the structures tend to be stable, and the final failure does depend on the materials strength. Evidently, given these fundamentally different failure modes in the cases of compressive and tensile loads, respectively, a combination of biaxial load conditions (compressive-compressive, compressive-tensile, tensile-compressive, and tensile-tensile) can lead to a quite complex behaviour and the need for developing predictive failure models that can account for this complexity.

2.1. Biaxial and multiaxial specimens

To generate useful strength data, a biaxial specimen must be capable of meeting a set of requirements [10],[11],[12],[13]: i) A sufficiently wide homogeneous biaxially-stressed zone must be generated for strain measurements, ii) Failure must occur within this zone. iii) No spurious loads (other than tension/compression) should be acting on the gauge specimen. iv) The specimen should accept arbitrary biaxial load ratios. The very design of specimens that recreate biaxially loaded components has become a constantly evolving field, aiming to provide optimal geometry, manufacture and general arrangement for a valid and reliable test [14]. Specimens designed for biaxial testing can be classified into three main groups: i) tubes, ii) thin plates and iii) cruciforms. A review of these groups and their main features is given below.

2.1.1. Tubular specimens

Multi-axial stress states were formerly created with thin-walled tubes subjected to internal pressure, torsion and axial loads [10],[11],[15]. These specimens allow simultaneous application of tensile and compressive longitudinal loads, as well as tangential and shear loads, therefore representing a versatile scheme for the conduction of multi-axial characterization (Figure 1).

However, the existence of stress gradients across the tubular wall makes this method less accurate than setups based on flat plates, which are also more representative of common industrial applications than the tubular geometry. Some studies also reveal high stress concentrations on the gripping ends. A further disadvantage is a pressure leakage after the onset of matrix failure, although some correction can be provided by internal linings [15].

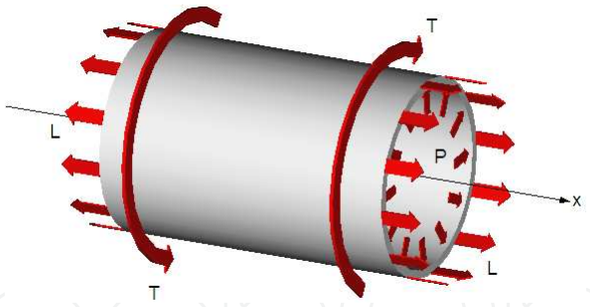

Figure 1. Thin-walled tube specimen.

2.1.2. Thin plates

Round or elliptical flat sheets subject to pressure in the hydraulic bulge test [16], as shown in Figure 2, can develop a biaxial stress state, although the technique has several disadvantages, for example, non-homogeneous stress distributions induced by gripping of the edges [17]. Also, just like the rhomboidal plate case, the loading ratio is shape-dependant [18] and can therefore not be varied during the test to obtain a full characterization.

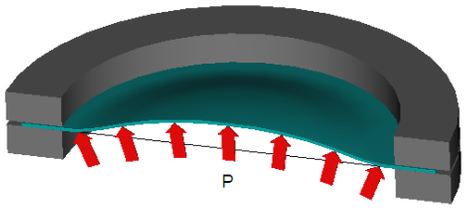

Figure 2. Elliptical flat sheet used in the bulge test.

2.1.3. Cruciform specimens

Testing biaxially-loaded cruciform specimens represent a more direct approach for obtaining true biaxial stress states, and consequently this method has gained wide acceptance [7],[8],[10],[11],[15]. As suggested by many researchers in the field [7],[10],[13], an ideal cruciform specimen should accomplish the following features: *i*) It should be capable of generating a sufficiently wide and homogenous biaxial stress/strain field in the gauge area, *ii*) failure must occur in the predefined gauge zone, *iii*) the cruciform should accept arbitrary biaxial load ratios for generating a complete failure envelope (within a desired range), *iv*) both the tested and the reinforcement layers should be of the same material, *v*) the transition between the gauge zone and the reinforced regions should be gradual enough as to avoid undesirable high stress concentrations, *vi*) the cruciform fillet radius should be as small as possible in order to reduce stress coupling effects, and *vii*) stress measurements in the test area should be comparable to nominal values obtained by dividing each applied load by its corresponding cross-sectional area. Although various cruciform geometries containing a central-square thinned gauge zone have been proposed in the literature, none can claim full satisfaction of the above requirements due to difficulties inherent to biaxial tests [10]. A cruciform with a thinned central region and a series of limbs

separated by slots is presented in Figure 3a. [19]; the slotted configuration allows greater deformations to occur in the thinned section, thus enforcing failure there. Nevertheless, thickness-change can induce undesirable stress concentrations that usually lead to premature failure outside the gauge zone. Also, the extensive machining required for thinning is an undesirable feature.

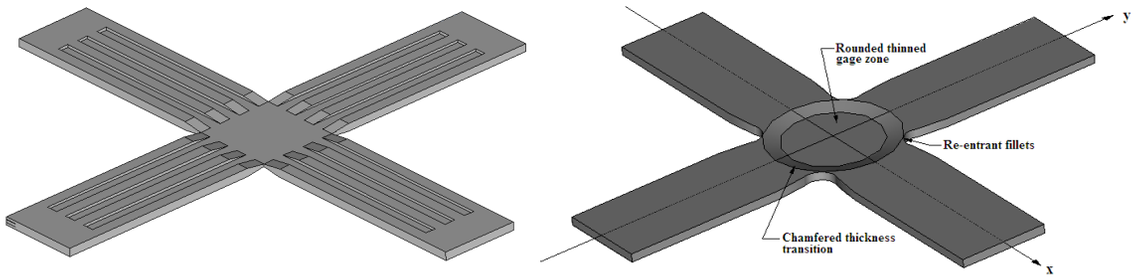

Figure 3. a). Slotted configuration[19] b). Thinned circular zone in the gauge zone [13].

Another cruciform, shown in Figure 3b, with a thinned circular zone in the gauge area [13] exhibits failure outside it, mainly because manufacturing defects caused unexpected higher strength in one axis. The implementation of a rhomboidal shaped test zone is suggested in [20], although, to the authors knowledge, no results with this geometry have been reported so far. Some experiments concluded that loading must be orthogonal to the fibre orientation to produce failure in the test zone [12]. The main difficulty in obtaining an optimal configuration is eliminating stress concentrations in the arms joints. To solve this, an iterative optimization process (numerical/experimental) yielded optimum geometric parameters of the specimen [21]. Results from this study led to a configuration characterized by a thinned square test zone and filleted corners between arms. Given that failure is prone to occur in the arms, reference [23] presented a design where a small cruciform slot is placed in the centre to cause load transfer from the arms to this region (figure 4a).

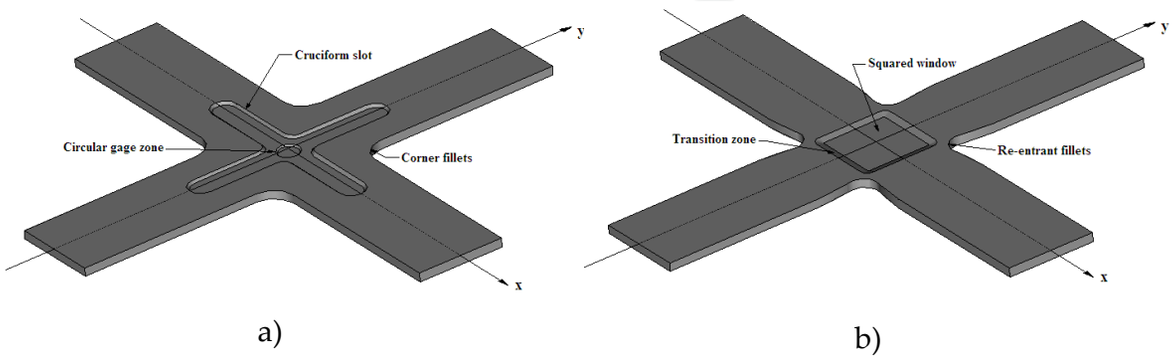

Figure 4. a). Inner cruciform slot [23]. b). Cruciform with thinned rounded square gauge zone and filleted corners [11].

Nevertheless the gauge zone is much reduced, and this makes this specimen useless for TC characterization. In the cruciform proposed by Ebrahim et al [10] failure in the gauge zone is

achieved. The design is characterized by a thinned rounded square gauge zone and considers a gradual thickness reduction in the biaxially loaded zone, and also filleted corners as shown in Figure 4b. Results were satisfactory, but it was found that the top and bottom edges of the depression presented high strain gradients. Based on the aforementioned references, a comprehensive study was conducted by the authors to obtain an improved cruciform design. A main feature of this new design is a rhomboid-shaped gauge zone which led to a much more homogeneous strain/strain distribution because of the alleviation of stress concentrations which occur in other designs due to the short distance between the gauge zone and the corners of the arms. Additionally, the corners are filleted to avoid another zone of stress concentration. The specimen is comprised of different layers where the inner layer is under study, whereas the outer ones (equal quantity on each side) are only for reinforcement.

2.1.4. Enhanced rhomboid-windowed cruciform specimen

In order to avoid premature failure due stress concentrations, a modified cruciform was proposed by considering this design concepts: i) Given that fillets are prime examples of stress concentrators, both the cruciform and gauge zone fillets should be as far apart as possible from each other, thus favouring a rhomboid-windowed gauge zone. This modification also intends to minimize regions of stress interactions, which cause lack of homogeneity in the strain field and even premature failure, as reported for some square-windowed specimens [22],[24]. Traditional (instead of re-entrant) fillets were preferred to maintain this stress concentrator as separated as possible from the gauge zone. ii) Since the focus of this research are textile composites (TC), the proposed specimen also features wider arms and a larger gauge zone, seeking to reduce the textile unit cell vs. gauge zone length ratio. This modification is in tune with ASTM standards on testing procedures for textile composites [25]. iii) To avoid polluting the obtained strength data with in-situ effects, adhesion between adjacent layers and other multilayer-related uncertainties, characterization is performed for a single-layer central gauge zone, while a number of reinforcement layers are added outside the gauge zone to enforce failure inside it. The resulting rhomboid windowed cruciform shape was similar to other specimens employed for fatigue characterization of ABS plastic, which report a smooth biaxial strain field at the gauge zone [26]. Basic dimensions were selected from a specimen reported in literature [27]: arm width w = 50mm and cruciform fillets R=25mm. The rhomboid window length l was set identical to the arm width, l=50mm while the window´s fillet radius r was set as 10% of l; the geometry is sketched in figure 5. Finite-element (FE) analysis demonstrated that this geometry generates a more uniform strain distribution, while the maximum shear strain in the cruciform fillet is relatively slow.

Once the suitability of a rhomboid windowed cruciform specimen for creating a biaxial strain state was established, a geometrical optimization process based on the experiment design methodology was conducted. Suitable objective functions were defined in order to homogenize the ε_x and ε_y strain fields inside the rhomboid gauge zone while maintaining shear strain γ_{xy} field close to zero. Details of the optimization process can be found in reference [29]

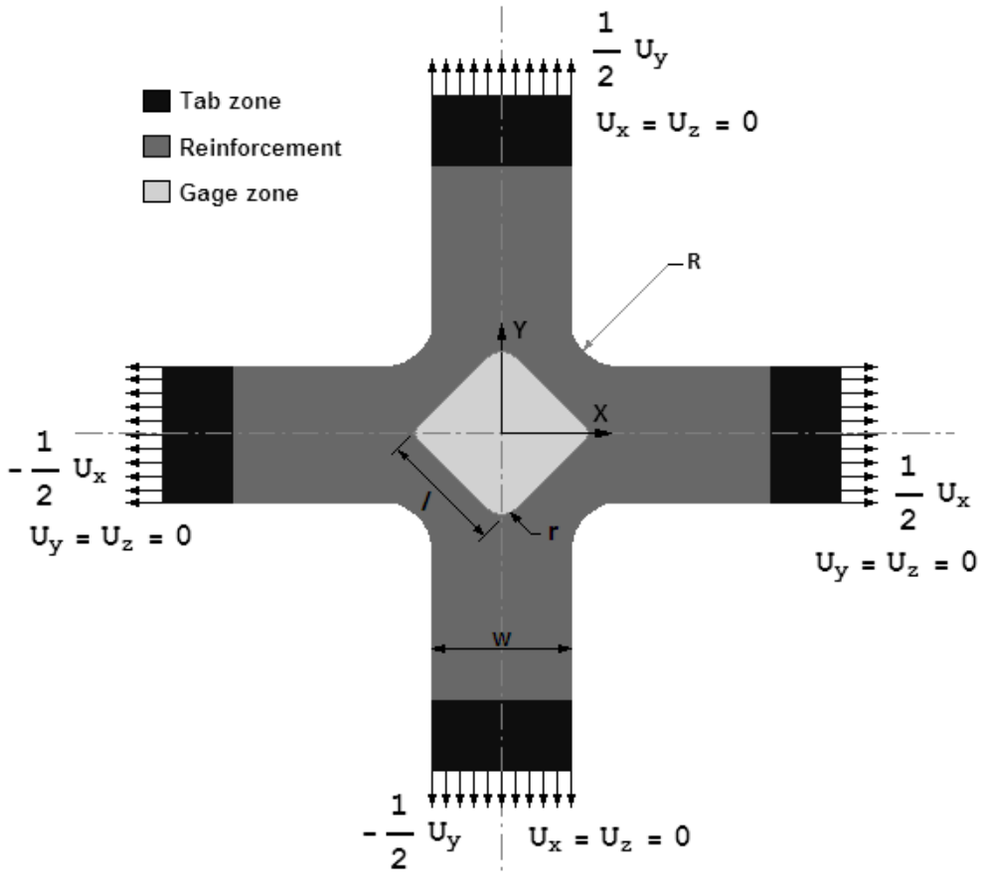

Figure 5. Geometry of the proposed cruciform specimen. Lay up for the reinforcement region is $[0]_5$, while for the gauge zone is [0] (that is, a single layer). All dimensions are given in mm.

E_{11}	[GPa]	25.0
E_{22}	[GPa]	25.0
v_{12}	[-]	0.2
G_{12}	[GPa]	4.0

Table 1. In-plane measured mechanical properties for a TC conformed of: Epoxy West System 105/206 reinforced with fibreglass cloth style #7520, bidirectional plain weave 8.5 oz./sq. yd, with 18L x 18W threads per inch count.

Evaluation of specimen using finite element analysis was carried by applying boundary conditions as defined in figure 5, with U_x and U_y chosen to produce a maximum strain (ε_x or ε_y) of 2% inside the gauge zone, corresponding to typical failure strain values reported for glass-epoxy TC [5]. The materials properties correspond to a generic plain weave bidirectional textile, as presented in Table 1.

The optimized geometry is defined in Figure 6, while the results of the FE analysis are shown in Figure 7, which splits the geometry into top and bottom sections for simultaneously illustrating the ε_x and γ_x strain fields, respectively, in a single graph; due to full symmetry, the ε_y strain field is identical to the ε_x field when rotated by 90°. The resulting geometry generates a very homogeneous strain field in the gauge zone and keeps shear strains near zero, while keeping shear strains in the fillet regions below the failure value.

These results are believed to represent a great improvement if compared with other specimens reported in the literature.

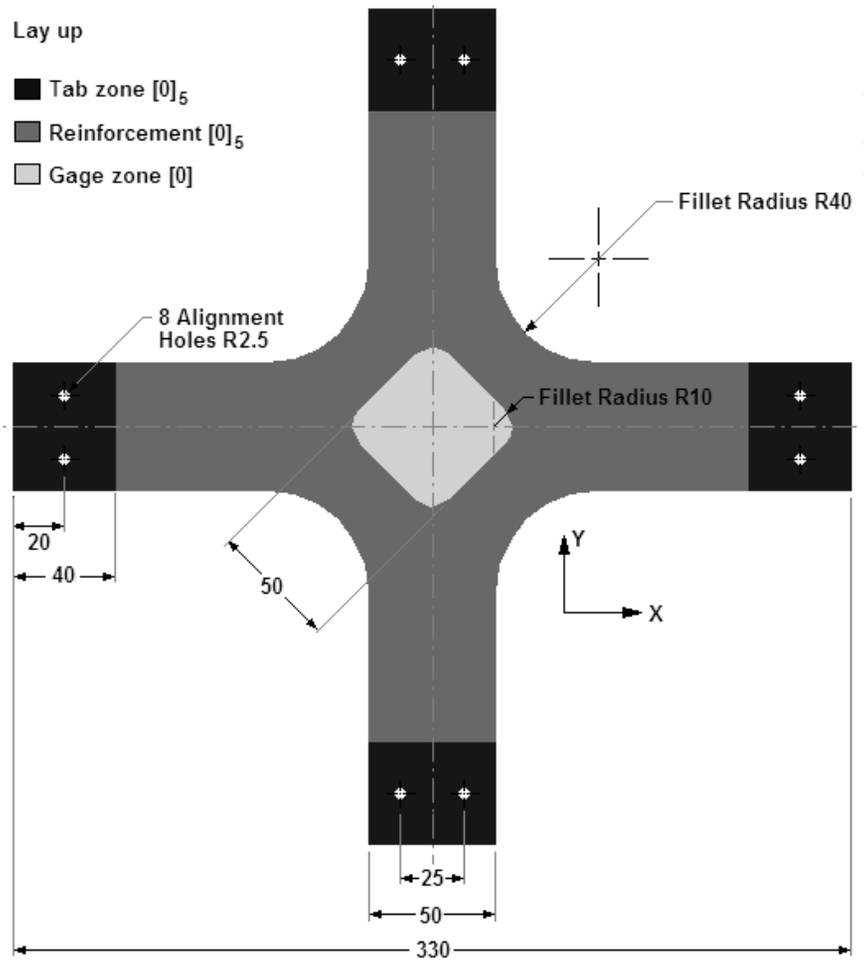

Figure 6. Optimized specimen specifications Dimensions are in mm.

2.2. Biaxial testing machines

To apply biaxial loads on cruciform specimens a specific device is required, which can meet the following requirements [28],[30],[12],[31]: i) The loads applied to a cruciform specimen must be strictly in tension or compression, avoiding spurious shear or bending loads. ii)The restriction previously stated implies that orthogonality among load axes must be guaranteed at all times during the test, and, consequently iii) the centre of the specimen must remain either still or the load axes must displace with it. An efficient method to ensure the previous condition is to apply equal displacements in the loaded axis. These requirements can be accomplished by using an active control system, or by passive mechanical methods, such that the one described later. A review of the most common biaxial testing systems is presented next.

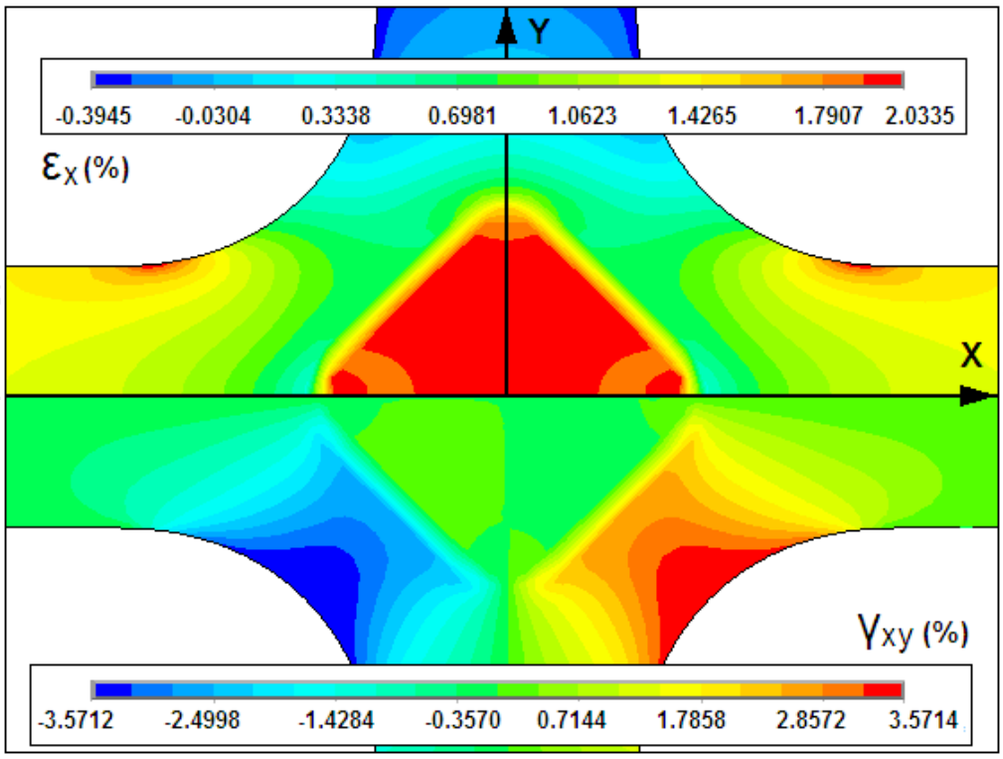

Figure 7. Linear strain field (upper part of the graph) and shear strain field (lower part) within and near the gauge zone of the optimized specimen.

2.2.1. Hydraulic systems

Hydraulic systems rely on hydraulic actuators to apply loads to the specimen; they typically use double-acting pistons with a closed-loop servo control system which sense displacements and/or loads as feedback, as implemented in the design by Pascoe and de Villiers [32]. This configuration (sketched on figure 8) which comprises the use of independent actuator for each applied load, allows the centre of the specimen to move during the test, which is an undesirable condition; this adverse feature can be avoided by implementing a control system that ensures synchronization of opposite actuators [33],[18] thereby avoiding motion of the centre of the specimen.

This configuration also allows the load ratios to be varied in order to obtain a full failure envelope. None of the systems mentioned could ensure equal displacement in both extremes of each axis, even the one using synchronization control, therefore allowing the centre of the specimen to move. If systems are implemented to correct this problem, the design and manufacturing costs inevitably increase. Fessler [34] proposed a machine in which motion is allowed only in one direction at one arm for each cruciform axis. This is the most common basic configuration found in the literature related to biaxial characterization of composites [35],[33]. In an attempt to simplify the previous concept while maintaining symmetric load conditions, some modifications have been proposed; for example, each loading axis, consisting of a pair of opposite hydraulic actuators, can be connected to a common hydraulic line so the force exerted by each side is the same and thus movements of the

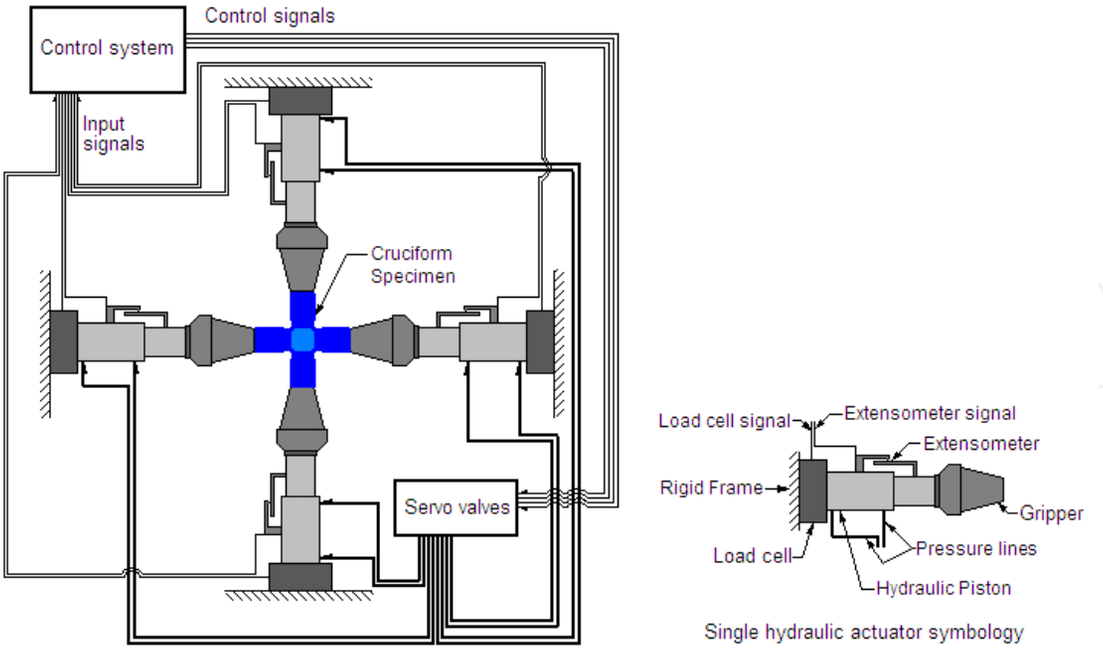

Figure 8. Use of independent actuator per load applied.

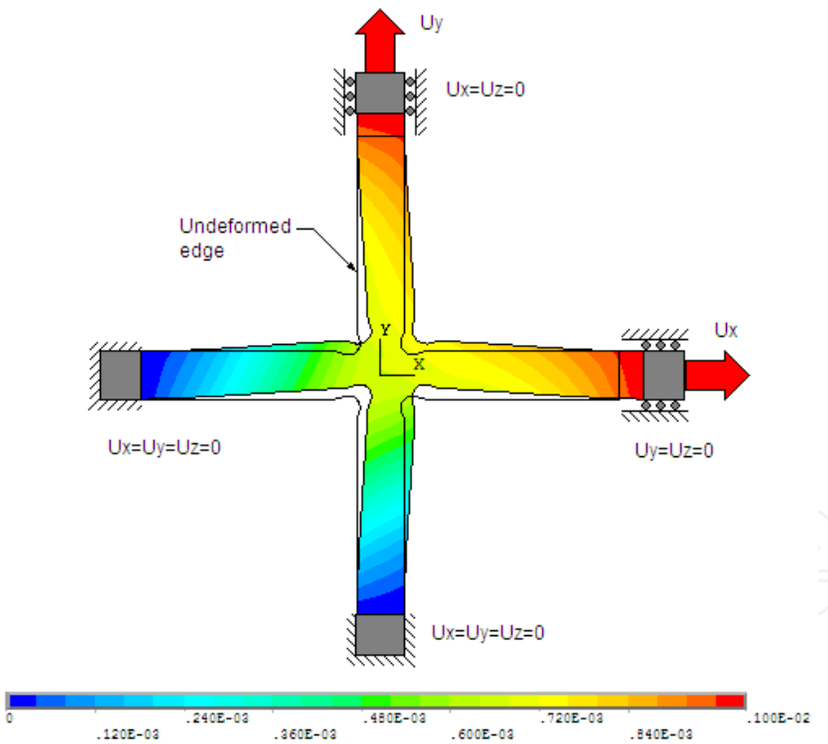

Figure 9. Contour plots of the magnitude of the displacement vector for the case of a configuration where one end of each axis is fixed and the other is displaced.

centre of the specimen are eliminated. Although the common hydraulic line ensures equal force in both extremes of one axis this does not ensure equal displacements. Another variation to hydraulic systems is described in the US Patent No. 5279166, which describes a biaxial testing machine consisting of two independently orthogonal loading axes capable of

applying tension and/or compression loads; two ends of the specimen are gripped to fixed ends while the complementary ends are fixed to grips attached to actuators that apply the load, made in an attempt to reduce the complexity and hence the costs of biaxial testing machines (fig. 9). This configuration results in significant displacements of the centre of the specimen, although it is stated that the machine has a mechanism that helps maintain the centre of the specimen and ensure that the loads are always orthogonal. In spite of these features, under large displacements the mechanism used is not capable of maintaining the orthogonally of the loads as shown by a quick finite-element evaluation, whose results are shown Figure 8; moreover, the resulting displacement field is completely asymmetric, a condition which generates undesirable shear stress. While most of the biaxial testing hydraulic machines are original developments, a commercial biaxial testing machine has been developed by the company MTS in conjunction with NASA. It uses four independent hydraulic actuators, each with a load cell and hydraulic grippers, and an active alignment system for the specimen. While solving most of the problems mentioned above, the cost of this system is too high for entry-level composites development laboratories.

2.2.2. Mechanical systems

Mechanical systems owe their name to the fact that they are based on the kinematics of their mechanisms to maintain load symmetry, no matter if the actuators are hydraulic or mechanic; even the application of deadweight to the specimen through systems of ropes, pulleys, levers and bearings has been considered, as presented by Hayhurst et al [36]. In practice, the mechanical systems proposed for the characterization of composite materials are mainly test rigs designed to be adapted to conventional uniaxial testing machines; basically, they are mechanisms consisting of coupled jointed-arms capable of applying in-plane biaxial loads to cruciform specimens. The load ratio is dependent on the geometrical configuration of the device [31] and can therefore be varied only by changing the length of one element, an impractical solution. Similar devices are found in French Patent No. 2579327 [37] and US Patent No. 7204160. A simpler mechanism is presented in US Patent No. 5905205 [30] which uses a four-bar rhomboid-shaped mechanism on which the loading ratios are changed before the test by certain variations in the assembly of the members. One of most practical mechanical systems found consist of four arms, joined at one side to a common block fixed via revolute joints to an universal test machine actuator through a load cell [26] which permits monitoring the applied force, while the other sides are linked, also with revolute joints, to a sliding block each; those blocks slide over a flat plate, fixed to the universal machine´s frame. The sliding blocks assemble the grippers which hold the specimen.

2.2.3. A novel biaxial testing apparatus

After reviewing the existing machines and mechanisms on which biaxial tests can be carried out, some conclusions can be drawn; in the case of some of them, the lack of a mechanism that automatically corrects any load difference that could lead to the displacement of the

centre of the specimen makes them unsuitable for reliable tests ; in those case where such mechanism does exist, it is controlled by means of an active system that increases design complexity and costs.

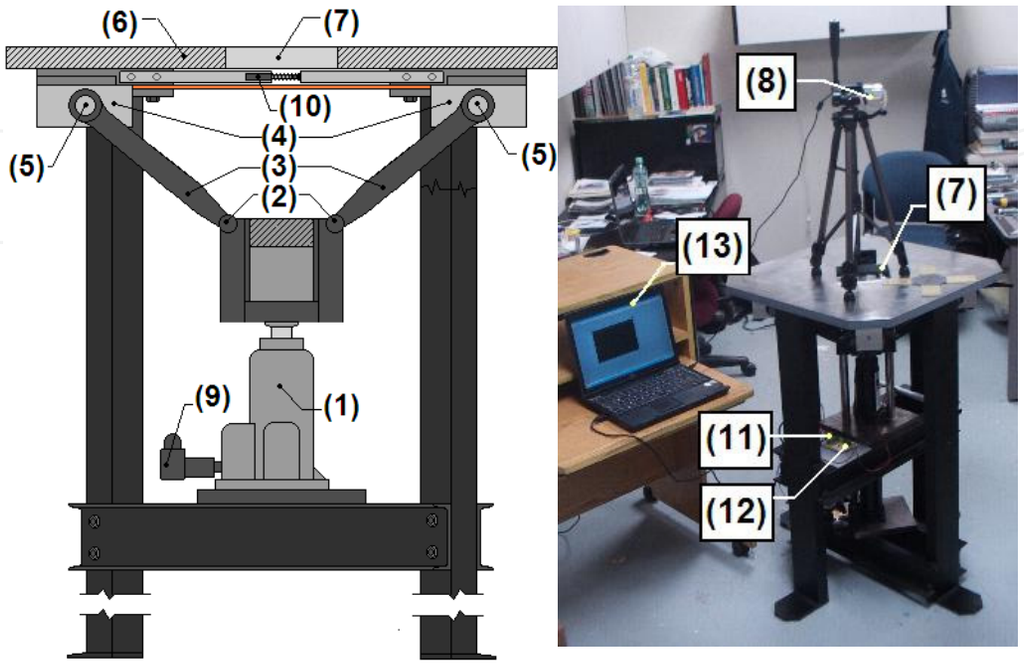

a. b.

Figure 10. a). Sketch of the biaxial testing machine, showing one load/displacement axis sketch. b). System general arrangement.

The design proposed by the authors considers these drawbacks, as well as the testing requirements previously stated; in addition, construction costs for the novel proposed design are considerably lower compared to other systems. The resulting apparatus is sketched in Figure 10a and a photograph of the completed machine in Figure 10b. The operational principles are described in the following (numbers in parentheses refer to the components identified in the corresponding figures): The loads are applied through a symmetrical slider-crank-slider mechanism meeting the following requirements: The hydraulic piston (1), which is the first slider, is attached on its base to the machine frame and provides the load drive, while its piston is linked by a revolute joint (2) to a pair of arms (3) arranged symmetrically, which in turn are connected by cylindrical joints (5) to the blocks where the grips holding the tab zone of the specimen are installed (4); these cylindrical joints allow to absorb small misalignment in the loads, as established in *iv*.

The grip blocks are lubricated and slide on the lower side of a flat plate (6) featuring a rectangular window (7) allowing a full-field view from the top of the machine, where a high-definition digital camera (HDDC) was installed (8), thereby satisfying the requirement *iii*. A similar arrangement was installed at a right angle with respect the first one, ensuring the independence of the load axes as required by *i*. Data acquisition is conducted by measuring the pressure in the hydraulic cylinders (9) and correcting this information by

considering the geometry of the mechanism, while the displacements are measured directly at the grips through resistive displacement sensors (10); all sensors are powered by a power board to provide a common voltage reference (11), and the signals are acquired through a National Instruments 8-channel analogical data acquisition board (12). The information was stored and processed on a laptop (13) by using a Lab View routine.

2.3. Data acquisition techniques

Unlike uniaxial tensile tests in which ultimate failure stress and strains data can be straightforwardly obtained from the collected load and displacement data, in the case of biaxial tests the strength values cannot be calculated directly in this way because the stress and strain fields are not necessarily homogeneous along the specimen and generally depend on the load in a non-trivial way due the complex geometry. For this reason biaxial testing requires a method capable of measuring the full strain field in the biaxially loaded zone of the specimen. Given that strain cannot be measured directly it is necessary to measure the displacement field, from which the strain field can be easily calculated. Using the strain field and a constitutive model the stress field can also be calculated. However, full-field measurement techniques are not standard data acquisition methods and in order to identify the most suitable technique for this research a survey was realized.

2.3.1. Full field strain measurement methods

The first method considered was reflective photo-elasticity; it is based on birefringence, a physical property which consists of the change of the refraction index of a material when shear stresses are applied. It has been used since decade of the 1950s [38], so is a well characterized technique. However, some limiting factors have been identified for the purposes of the curent project: 1) The preparation of the samples is extremely laborious and requires the application of a layer of birefringent material on the surface to be observed, with a thickness of a few millimetres [38].If compared with the thickness of the composite layer under study which is of the orderof about 0.2-0.3mm it is clear that the application of the measurement layer significantly affects the test results. Another technique considered was Moiré interferometry. This technique requires the printing of a pattern of lines on a transparent medium, which is then illuminated by a LASER source, generating an interference pattern which depends on the deformation of the specimen [39]. However, this method has the disadvantage that the data reduction process is tedious and complex [40], and the results heavily depend on the analyst's experience. After considering these options, a technique called digital image correlation (CDI) was identified from biaxial testing literature [10], [11], [41]. The basic concept consists of obtaining digital images of studied geometry on it initial, non-deformed state and after being subjected to a deformation. The surface of the part under study is pre-printed with a random speckle pattern, so that the displacements between corresponding points on photographs of the non-deformed and deformed states, respectively, can be identified by a computer algorithm. This method has some advantage over the ones mentioned above [42]:

i) The experimental setup and specimen preparation are relatively simple; only one fixed CCD camera is needed to record the digital images of the test specimen surface before and after deformation. ii) Low requirements as to the measurement environment: 2D DIC does not require a laser source. A white light source or natural light can be used for illumination during loading. Thus, it is suitable for both laboratory and field applications. iii) Wide range of measurement sensitivity and resolution: Since the 2D DIC method deals with digital images, the digital images recorded by various high spatial-resolution digital image acquisition devices can be directly processed by the 2D DIC method. For the reasons stated above the 2D DIC method is currently one of the most actively used optical measurement techniques and demonstrates increasingly broad application prospects. Nevertheless, the 2D DIC method also has some disadvantages: i) The surface of the planar test object must have a random grey intensity distribution. ii)The measurements depend heavily on the quality of the imaging system. iii) At present, the strain measurement accuracy of the 2D DIC method is lower than that of interferometric techniques, and is not recommended for the measurement of very small and non-homogeneous deformations. Despite these restrictions the low cost associated with equipment and the low specimen preparation requirements makes Digital Image Correlation the preferred technique for the purposes of this study. The drawbacks can be largely avoided by using the highest-definition camcorder commercially available, using an established Digital Image Correlation program and using a specimen that generates a relatively homogeneous strain field. It was shown above that by proper design and optimization a very homogeneous strain field can indeed be obtained in the gauge zone, so this restriction of the DIC technique was of no concern to this project. Finally, the expected strain values were large enough to be safely detected by the DIC technique.

3. Experimental setup

3.1. Specimen manufacture

As stated by recent research [11] the milling process typically employed to thin the gauge zone produces undesirable damage and stress concentrations in unidirectional (UD) composites; for textile composites (TC), milling would exacerbate this problem due to its more complex 3D structure, making milling an unacceptable choice. The main concern is to preserve the integrity of the textile structure, especially when characterizing a single lamina. To generate a damage-free cruciform specimen with a single-layered gauge zone, a novel manufacturing process was developed by the authors, explained below: **1).** Non-impregnated fabric sheets were fixed to a 6mm thick plywood base to ensure dimensional stability, with a printed grid to help proper fibre alignment of each cloth. The whole arrangement was cut into a square pre-form using a water jet, also cutting away the rhomboidal window corresponding to the gauge zone, as shown in the Figure 11. Afterwards, the material was oven-dried at 60°C during 12 hours to eliminate moisture.

2) The following numeric values inside brackets refer to indications given in Figure 12. Two reinforcement layers (1) corresponding to the bottom side of the cruciform specimen were placed in a lamination frame, consisting of a flat surface (2) surrounded by a square border

(3) with a side length equal to that of the specimen. A pre-formed 2-layer rhomboid step (4) was located at the centre, corresponding to the location of the gauge zone, to ensure planarity of the central layer (5). The reinforcement layers were manually resin-impregnated and, immediately after this, the central layer (5) was placed and impregnated. Finally, the process was repeated for the last two reinforcement layers (6), as shown. Room environment was controlled during the lamination process at a temperature of 80±2°C and 50-60% relative humidity. Immediately after the impregnation process was completed, the laminate was placed in a vacuum bag consisting of a peel ply (7), perforated film (8), bleeder cloth (9) and the bag itself (10), using sealing tape to ensure vacuum seal (11). 0.8 bar vacuum pressure was applied through a valve located at a corner (12), sufficiently away from where the final shape would be cut. The whole arrangement was cured during 4 hours inside a pre-heated oven at 80±2°C, as measured by a thermo-couple (13) located at the gauge zone, as shown in Figure 12. **3)** After curing, the final cruciform geometry was obtained through water jet cutting. Nine specimens were prepared meeting the dimensional specifications in Figure 6.

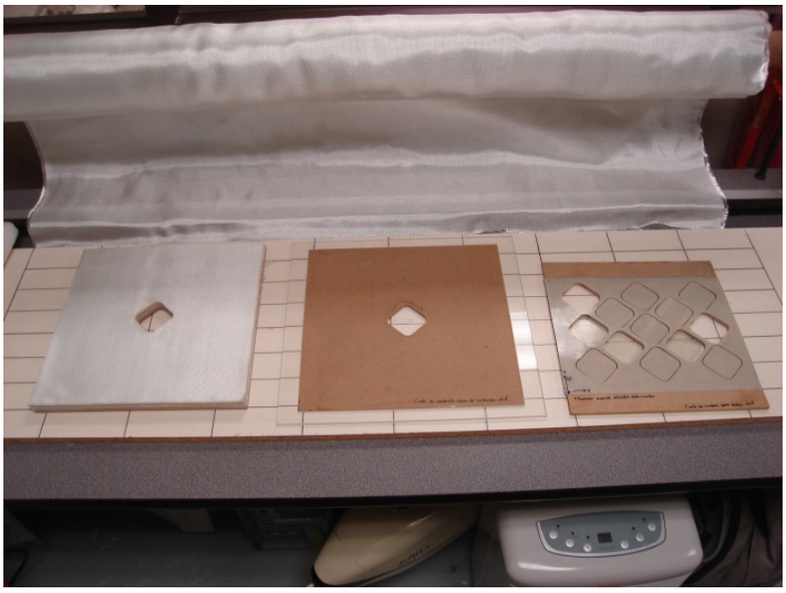

Figure 11. Rhomboid window cutted on the reinforcement layers and other auxiliary tools.

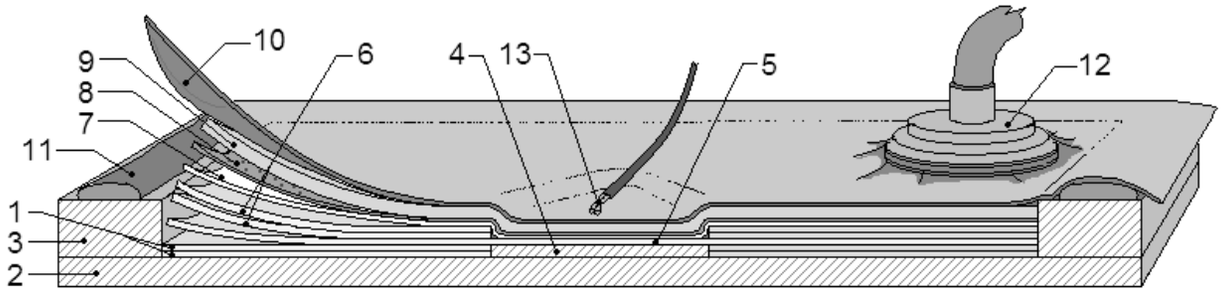

Figure 12. Arrangement for specimen manufacture.

To provide visual reference for the digital image correlation (DIC) strain field measurement [24][41], specimens were painted with a black-dot random speckle pattern over a white-mate primer, as shown in Figure 13. This technique was preferred over the spraying

technique reported in [41], as it might result in an inadequate control of the dot size distribution, leading to uncertainty in the DIC measurements. Additionally, five uniaxial, $[0]_5$ layup specimens were prepared in order to perform uniaxial tests to provide precise input data for the development of failure criteria.

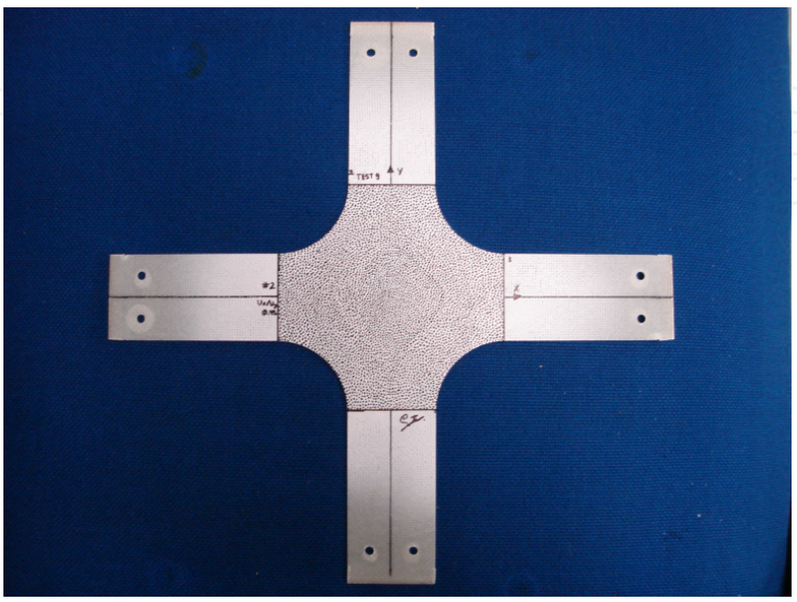

Figure 13. Finished specimen exhibiting its speckle pattern used with the digital image correlation technique

3.2. Biaxial testing

Experimental validation of the optimized cruciform was conducted with the biaxial testing apparatus described in section 2.2.3 as follows: after mounting the specimen in the grippers, a pre-load of 500N was applied to each axis prior to tightening the mounting bolts. (Figure 14) Then, preload and alignment bolts were removed, setting the measured displacements and loads to zero. A high-quality video of the specimen was recorded with a high definition cam coder with adjustable focus and exposure parameters functions for subsequent DIC analyses.

A chronometer synchronized with the computer clock was placed near the specimen and inside the camera vision field, to ensure its inclusion in the captured images; this provided a time reference to relate each video frame with correspondent load data. After starting video recording and the data capture routine, biaxial displacements were applied at a rate of 1mm/min until final failure. This load rate was selected based on the ASTM 3039 standard [43], which recommends a displacement speed such that failure occurs 1 to 10 minutes after the start of the test.

Data acquisition and reduction was conducted as follows: two video frames were taken from the recorded video sequence, one corresponding to the beginning of the test and another just prior to final failure, as shown in figure 15. Both images were fed into the open access software DIC2D (developed by Dr. Wang's team at the Catholic University of America) to obtain the full strain field (ε_x , ε_y and γ_{xy}). The three tests performed covered a

range of biaxial ratio BR values in the vicinity of the critical condition BR=1: BR=1.5 (Test #1), BR=1.25 (Test #3), and BR=1 (Test #5). Figure 15 shows the final failure sequence representative of the tests conducted. It should be noted that the failure occurred well within the gauge zone as expected from the FE-predicted strain fields.

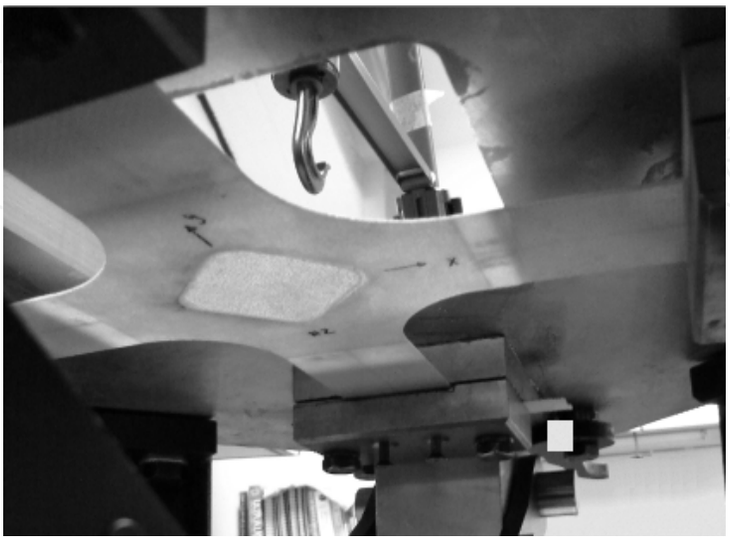

Figure 14. Cruciform specimen mounted in the biaxial testing machine.

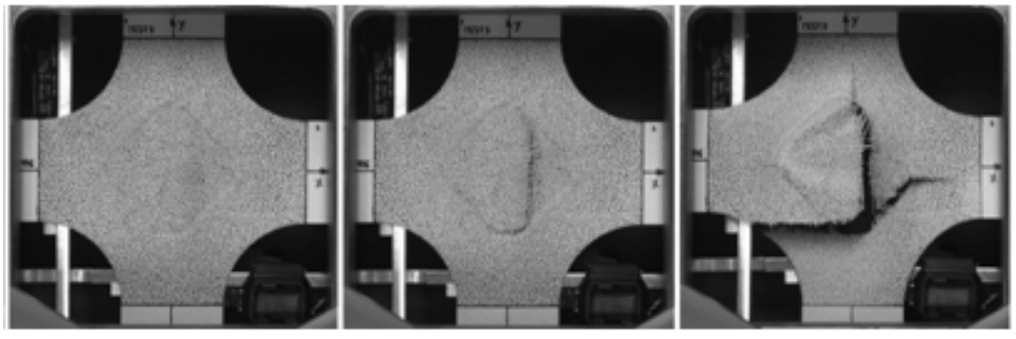

Figure 15. Final failure sequence recorded at 30 frames per second.

The final failure is clearly fibre-dominated, due to its catastrophic nature; it is possible to identify the final failure onset region inside the rhomboidal gauge zone, as required for a successful test. Regarding the strain field, it can be seen from Figure 16 that the agreement between the experimentally results (obtained from DIC) and the FE prediction is remarkably good. The DIC and the FE images show the same symmetry of the experimental shear strain pattern and similar homogeneity and smoothness, and the absolute strain values cover a similar range. This can be considered an additional indicator of the success of the experimental procedure presented in this work.

The same procedure used to characterize the ultimate strain can be used to obtain the matrix onset failure envelope (as opposed to fibre failure), but due to the fact that this phenomenon cannot be deduced visually a different approach was used for this purpose. The load vs. displacement plots were used to identify the change in the slope which evidences matrix damage, as shown in the Figure 17. This method is proposed as an extrapolation of the

method employed for uniaxial tests defined by the ASTM 3039 standard for the uniaxial tensile characterization of composites [43]. Linear fits were obtained for every linear segment of curves corresponding to every perpendicular axis, and the intersections were calculated solving the resulting equations, which allowed to quantify the strain values corresponding to the onset of matrix damage, considering that the latter occurs at the first observed slope change. Once the displacement and strain were identified, the digital image corresponding were used to perform a DIC analysis and to get the full field strain in the same fashion described previously.

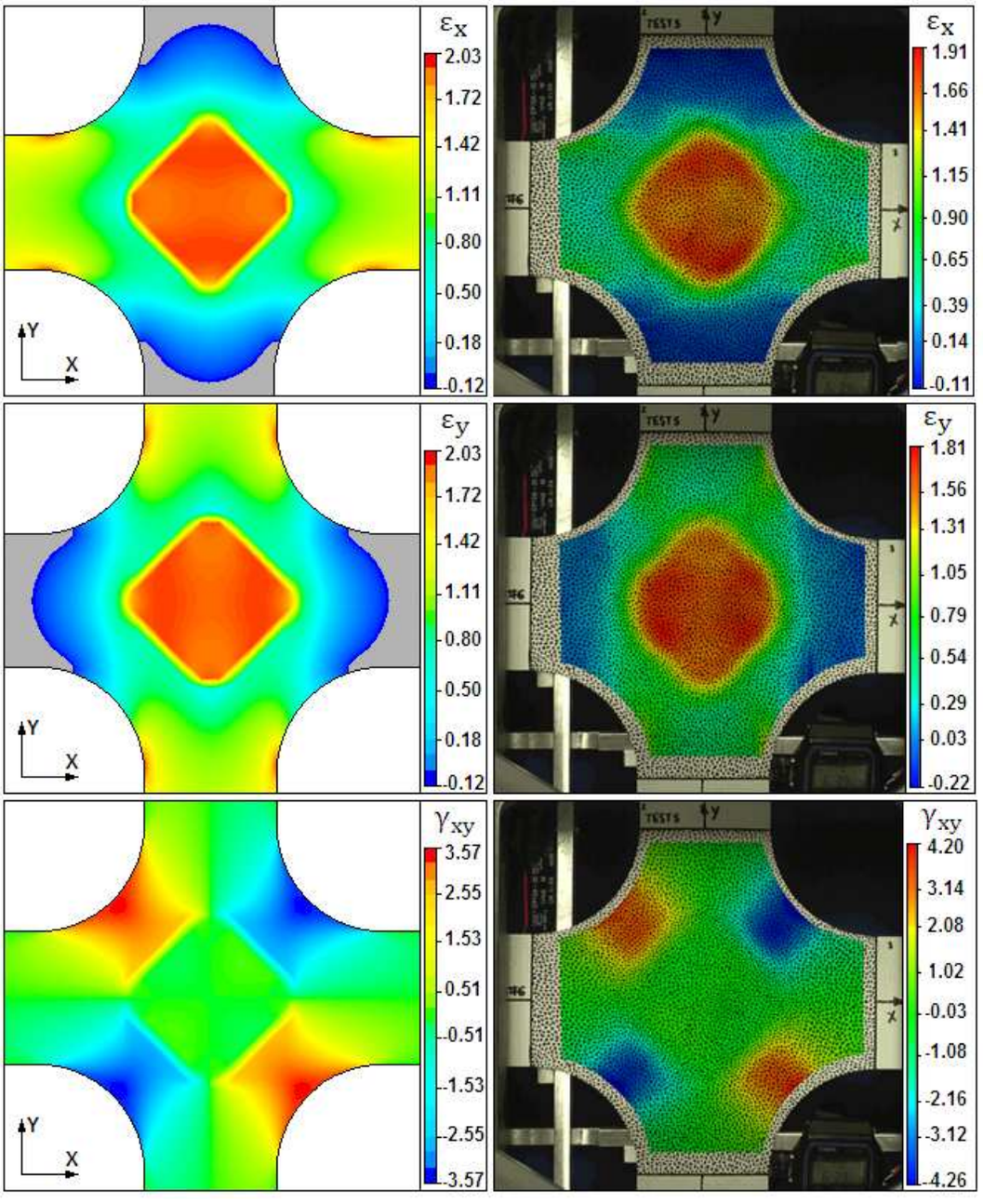

Figure 16. FE vs DIC strain field comparison for Test #5. The first column corresponds to the FE results, while the second column exhibits the results of the digital image correlation (DIC) process. The first and second row show the linear strain field, while the last row exhibits the shear strain stress field.

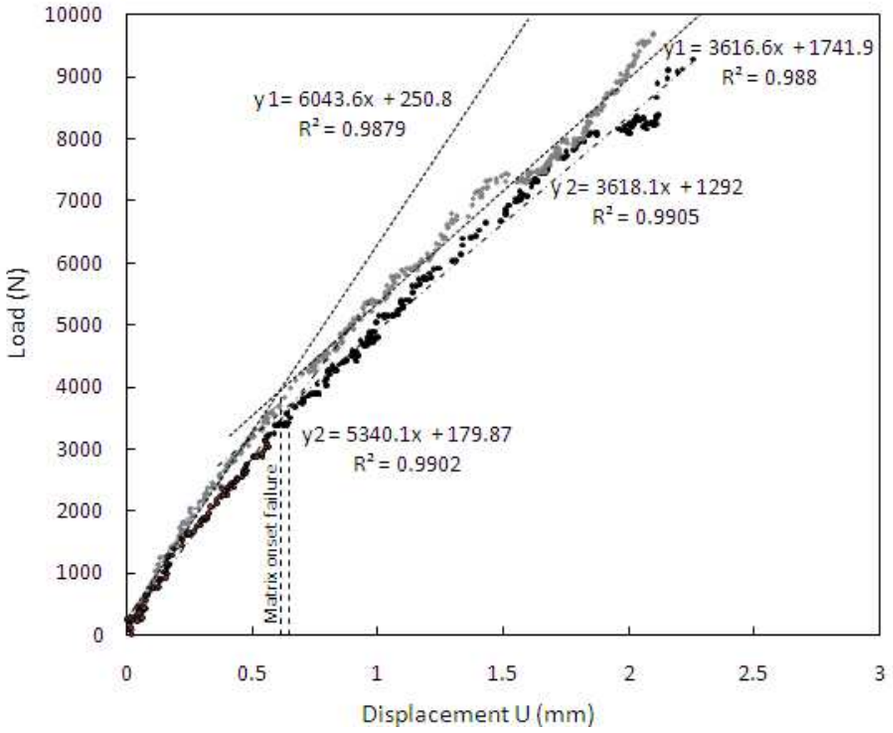

Figure 17. Load vs diplacement for biaxial test #3. The location where the change of slope occurs is interpreted as the onset of matrix failure.

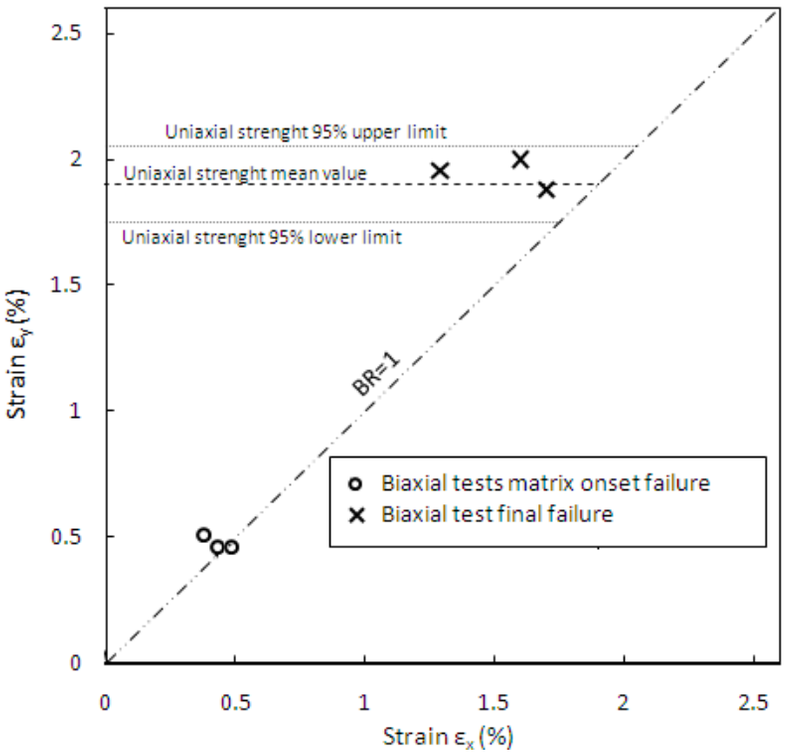

Figure 18. Failure envelope data obtained from the experimental data

Is important to remark that the use of the slope change in the load vs. displacements curves can be significantly influenced by geometrical effects and materials non-linearity, and other

auxiliary techniques such as sonic emission or in-situ x-ray scanning should be employed to verify that this change can be effectively used as a matrix damage onset indication.

Experimental strength data for single layer biaxial strength obtained from the experimental program are presented in Figure 18 as well as data from uniaxial test performed on five layer specimens. Confidence intervals calculated for the failure strains observed on uniaxial tests are presented in the figure. It should be noted that single-layer strength data fall inside the 95% confidence limits which suggest that interactions between ε_1 and ε_2 strains are significant for single layer laminates. This finding should not be used as design criterion before more experimental data are obtained, but it gives a good indication of the feasibility of the methodology presented for the purposes of failure analysis.

4. Conclusions

Improvement over existing cruciform specimens for biaxial testing was achieved by proposing a specimen with rhomboidal thinned gauge zone, based on conclusions from a qualitative stress concentration analysis. An optimization based on the experiment design methodology was performed to achieve a highly homogeneous strain distribution withinu the rhomboidal gage zone while shear strains in the cruciform fillets were kept well below the failure values in order to avoid the premature failure typically affecting this kind of specimens. The resulting geometry generates very homogeneous strain field within the gauge zone and keeps shear strains near zero, while keeping shear strains in fillets below the failure value; this is believed to represent a great improvement over other specimens reported in the literature. In addition to meeting the requirements for equi-biaxial tests, the specimen was evaluated under various biaxial ratios, demonstrating that is practically insensitive to biaxial ratio, and hence can be used without any modification to obtain the full tension-tension failure envelope.

A manufacturing process which avoids machining operations normally required to generate the thinned gauge zone was developed, in an attempt to preserve the textile architecture from machining micro-damage. It consists in cutting the rhomboidal windows from the reinforcement layers prior to its matrix impregnation by using a water jet cutting machine. Despite the highly manual work involved in the specimens manufacturing process, it measured specifications were according to those extrapolated from ASTM 3039 for composite materials unidirectional samples.

Validation of the specimen's geometry and manufacturing technique was made through experimental testing, which were conducted on the in-house-developed biaxial machine. The cruciform´s full strain field was measured via digital image correlation; the results demonstrate, in close agreement with the results obtained from finite-element(FE) simulations, that the specimen generates a significantly more homogeneous biaxial load state in the gauge zone than others reported in literature, and failure occurs, for all the tests, inside the gauge zone, as intended.

Author details

David Alejandro Arellano Escárpita*, Diego Cárdenas,
Hugo Elizalde and Ricardo Ramirez
Mechatronics Engineering Department, Instituto Tecnológico y de Estudios Superiores de Monterrey, Campus Ciudad de México, Col. Ejidos de Huipulco, Tlalpan, México D.F., Mexico

Oliver Probst
Physics Department, Instituto Tecnológico y de Estudios Superiores de Monterrey, Campus Monterrey, Monterrey, N.L., Mexico

5. References

[1] Crookston JJ, Long AC, Jones IA. A summary review of mechanical properties prediction methods for textile reinforced polymer composites. Proceedings of the Institution of Mechanical Engineers, Part L: Journal of Materials: Design and Applications 2005; 219(2):91-109.

[2] Soden PD, Kaddour AS, Hinton M.J. Recommendations for designers and researchers resulting from the world-wide failure exercise. Composites Science and Technology 2004; 64(3-4): 589–604.

[3] Kaddour AS, Hinton MJ. Instructions To Contributors Of The Second World-Wide Failure Exercise (Wwfe-II): Part(A).

[4] Lomov SV, Huysmans G, Luo Y, Parmas RS, Prodromou A, Verpoest I, Phelan FR. Textile composites: modelling strategies. Composites: Part A 2001; 32(10): 1379-1394.

[5] Welsh JS, Mayes JS, Key CT, McLaughlin RN. Comparison of MCT failure prediction techniques and experimental verification for biaxially loaded glass fabric-reinforced composite laminates. Journal of Composite Materials 2004; 38(24):2165-2181.

[6] Swanson SR, Smith LV. Comparison of the biaxial strength properties of braided and laminated carbon fibre composites. Composites: Part B 1996; 27(1):71-77.

[7] Welsh JS, Adams DF. An experimental investigation of the biaxial strength of IM6/3501-6 carbon/epoxy cross-ply laminates using cruciform specimens. Composites: Part A 2002; 33(6):829-839.

[8] Welsh JS, Mayes JS, Biskner A. 2-D biaxial testing and failure predictions of IM7/977-2 carbon/epoxy quasi-isotropic laminates. Composite Structures 2006; 75(1-4):60-66.

[9] Ng RK, Yousefpour A, Uyema M, Ghasemi MN. Design, Analysis, Manufacture, and Test of Shallow Water Pressure Vessels Using E-Glass/Epoxy Woven Composite Material for a Semi-Autonomous Underwater Vehicle. Journal of Composite Materials 2002; 36(21): 2443-2478.

* Corresponding Author

[10] Ebrahim L, Van Paepegem W, Degrieck J, Ramault C, Makris A, Van Hemelrijck D. Strain distribution in cruciform specimens subjected to biaxial loading conditions. Part 1: Two-dimensional versus three-dimensional finite element model. Polymer Testing 2010; 29(1):7-13.

[11] Ebrahim L, Van Paepegem W, Degrieck J, Ramault C, Makris A, Van Hemelrijck D. Strain distribution in cruciform specimens subjected to biaxial loading conditions. Part 2: Influence of geometrical discontinuities. Polymer Testing 2010; 29(1):132-138.

[12] Fawaz, Z. Étude analytique, numérique et expérimentale portant sur la rupture et la fatigue biaxiales des lamelles renforcées de fibres. PhD Thesis, Sherbrooke: Université de Sherbrooke, 1992.

[13] Gupte AA. Optimization of Cruciform Biaxial Composite Specimen. In: Master on Science Thesis. South Dakota State University, 2003.

[14] Sepúlveda CG. Biaxial Testing of Composite Materials: Technical Specifications and Experimental Set-up *Maestría en Ciencias con Especialidad en Sistemas de Manufactura* México Mayo 2009

[15] Soden PD, Hinton MJ, Kaddour AS. Biaxial test results for strength and deformation of a range of E-glass and carbon fibre reinforced composite laminates: failure exercise benchmark data. In: Failure Criteria in Fibre Reinforced Polymer Composites: the World-Wide Failure Exercise. Oxford: Elsevier Science LTD, 2004, p. 52-96.

[16] Bird JE, Duncan J. Strain hardening at high strain in aluminum alloys and its effect on strain localization. Metallurgical and Materials Transactions A 1981; 12(2): 235-241.

[17] Dudderar TF, Koch, Doerries DE. Measurement of the shapes of foil bulge-test samples. Experimental Mechanics 1977; 17(4): 133-140.

[18] Boehler JP, Demmerle S, Koss S. A New Direct Biaxial Testing Machine for Anisotropic Materials. Experimental Mechanics 1944; 34(1): 1-9.

[19] Mönch, E., and D. Galster. "A Method for Producing a Defined Uniform Biaxial Tensile Stress Field." British Journal Of Applied Physics 14, no. 11 (1963).

[20] Sacharuk, Z. Critères de rupture et optimisation des éléments en matériaux composites. PhD Thesis. Université de Sherbrooke. Sherbrooke 1990

[21] Youssef, Y. Résistance des composites stratifiés sous chargement biaxial: validation expérimentale des prédictions théoriques. PhD Thesis, Sherbrooke: Université de Sherbrooke, 1995.

[22] Arellano D, Sepúlveda G, Elizalde H, Ramírez R. "Enhanced cruciform specimen for biaxial testing of fibre-reinforced composites." International Materials Research Congress. Cancun, 2007.

[23] Yong Yu, Min Wan, Xiang-Dong Wu, Xian-Bin Zhou. Design of a cruciform biaxial tensile specimen for limit strain analysis by FEM. Journal of Materials Processing Technology 2002; 123:(67-70)

[24] Antoniou AE, Van Hemelrijck D, Philippidis P. Failure prediction for a glass/epoxy cruciform specimen under static biaxial loading. Composite Science and Technology 2010; 70(8):1232-1241.

[25] ASTM Standard D6856–03, Standard Guide for Testing Fabric-Reinforced Textile Composite Materials, 2003.

[26] Kwon HJ, Jar PYB, Xia Z. Characterization of bi-axial fatigue resistance of polymer plates. Journal of Materials Science 2005; 40(4):965– 972.

[27] Gdoutos EE, Gower M, Shaw R, Mera R. Development of a Cruciform Specimen Geometry for the Characterisation of Biaxial Material Performance for Fibre Reinforced Plastics. Experimental Analysis of Nano and Engineering Materials and Structures. Springer Netherlands, 2007. p. 937-938.

[28] [28] Chaudonneret M, Gilles P, Labourdette R, Policella H. Machine d'essais de traction biaxiale pour essais statiques et dynamiques. La Recherche Aérospatiale 1977:299-305.

[29] David Alejandro Arellano Escárpita. Experimental investigation of textile composites strength subject to biaxial tensile loads. Ph.D. Thesis. Instituto Tecnológico y de Estudios Superiores de Monterrey. Monterrey 2011.

[30] Clay SB. Biaxial Testing Apparatus. United States of America Patent 5905205. 18 May 1999.

[31] Ferron G, Makinde A. Design and Development of a Biaxial Strength Testing Device. Journal of Testing and Evaluation (ASTM) 16, no. 3 (May 1988).

[32] [32] Pascoe KJ, de Villiers JWR. Low Cycle Fatigue of Steels Under Biaxial Straining. Journal of Strain Analysis 1967; 2(2).

[33] Welsh JS, Adams DF. Development of an Electromechanical Triaxial Test Facility for Composite Materials. Experimental Mechanics 2000; 40(3): 312-320.

[34] Fessler H, Musson JK. A 30 Ton Biaxial Tensile Testing Machine. Professional Engineering Publishing 1969; 4(1): 22-26.

[35] Makinde A, Thibodeau L, Neale K. Development of an apparatus for biaxial testing using cruciform specimens. Experimental Mechanics 1992; 32(2): 138-144.

[36] Hayhurst DR. A Biaxial-Tension Creep-Rupture Testing Machine. Professional Engineering Publishing 1973; 8(2): 119-123.

[37] Ferron, G. Dispositif perfectionné d'essais de traction biaxiale. France. 26 Septembre 1986.

[38] Doyle JF, Phillips JWP. Manual on experimental stress analysis. Society for Experimental Mechanics (U.S.). Society for Experimental Mechanics, 1989.

[39] Post D, Han B. Chap 22, “Moire Interferometry,” Handbook on Experimental Mechanics, W. N. Sharpe, Jr., ed., Springer-Verlag, NY, 2008.

[40] Gre´diac M. The use of full-field measurement methods in composite material characterization: interest and limitations. Composites: Part A 2004; 35(7-8):751-761.

[41] Lecompte D, Smits A, Bossuyt S, Sol H, Vantomme J, Van Hemelrijck D, Habraken AM. Quality assessment of speckle patterns for digital image correlation. Optics and Lasers in Engineering 2006; 44(11):1132-1145.

[42] Bing P, Kemao Q, Huimin X, Anand A. Two-dimensional digital image correlation for in-plane displacement and strain measurement: a review. Measurement Science and Technology 2009; 20(6): 1-17.
[43] ASTM Standard D 3039/D 3039M, Standard Test Method for Tensile Properties of Polymer Matrix Composite Materials, 2000.